Bioluminescence Methodology for the Detection of Protein–Protein Interactions Within the Voltage-Gated Sodium Channel Macromolecular Complex

Alexander Shavkunov,[1] Neli Panova,[1] Anesh Prasai,[1] Ron Veselenak,[2,3] Nigel Bourne,[2,3] Svetla Stoilova-McPhie,[4,5] and Fernanda Laezza[1]

Departments of [1]Pharmacology and Toxicology, [2]Pediatric Vaccinology, and [4]Neuroscience and Cell Biology, and [5]Sealy Center for Structural Biology and Molecular Biophysics, University of Texas Medical Branch, Galveston, Texas. [3]Assay Development Service Division, Galveston National Laboratory, Galveston, Texas.

ABSTRACT

Protein–protein interactions are critical molecular determinants of ion channel function and emerging targets for pharmacological interventions. Yet, current methodologies for the rapid detection of ion channel macromolecular complexes are still lacking. In this study we have adapted a split-luciferase complementation assay (LCA) for detecting the assembly of the voltage-gated Na^+ (Nav) channel C-tail and the intracellular fibroblast growth factor 14 (FGF14), a functionally relevant component of the Nav channelosome that controls gating and targeting of Nav channels through direct interaction with the channel C-tail. In the LCA, two complementary N-terminus and C-terminus fragments of the firefly luciferase were fused, respectively, to a chimera of the CD4 transmembrane segment and the C-tail of Nav1.6 channel (CD4-Nav1.6-NLuc) or FGF14 (CLuc-FGF14). Co-expression of CLuc-FGF14 and CD4-Nav1.6-NLuc in live cells led to a robust assembly of the FGF14:Nav1.6 C-tail complex, which was attenuated by introducing single-point mutations at the predicted FGF14:Nav channel interface. To evaluate the dynamic regulation of the FGF14:Nav1.6 C-tail complex by signaling pathways, we investigated the effect of kinase inhibitors on the complex formation. Through a platform of counter screenings, we show that the p38/MAPK inhibitor, PD169316, and the IκB kinase inhibitor, BAY 11-7082, reduce the FGF14:Nav1.6 C-tail complementation, highlighting a potential role of the p38MAPK and the IκB/NFκB pathways in controlling neuronal excitability through protein–protein interactions. We envision the methodology presented here as a new valuable tool to allow functional evaluations of protein–channel complexes toward probe development and drug discovery targeting ion channels implicated in human disorders.

INTRODUCTION

Rapid progress in the complementary fields of molecular genetics and proteomics has led to the appreciation of protein–protein interactions within macromolecular complexes as key determinants of ion channel functional modulation.[1,2] These macromolecular complexes play a critical role in regulating biophysical properties, surface expression, and membrane localization of channels through highly specific contact surfaces.[2,3] The specificity of these protein–channel interactions usually resides in a few critical amino acid residues at the interface, referred to as "hot spots." An emerging concept in the field of ion channel research is to leverage these hot spots as new targets for drug development.[4,5] Yet, the ever growing number of protein–protein interactions poses a challenge in target selection. We propose that functional significance of the target and availability of structural information on the protein–channel complex are likely to provide the fundaments for a successful drug discovery campaign, facilitating hit-to-lead transition (structural information) and preclinical testing (functional significance).

Voltage-gated Na^+ (Nav) channels are heteromeric transmembrane proteins consisting of a pore-forming α-subunit (Nav1.1–Nav1.9) and accessory β-subunits (β_1 to β_4); these channels are activated by membrane depolarization giving rise to action potentials and providing the basis for excitability in neurons and cardiomyocytes.[6] Recent discoveries indicate that intracellular fibroblast growth factor 14 (FGF14) is a biologically relevant component of the Nav channel macromolecular complex. FGF14 is a member of the

ABBREVIATIONS: AIS, axonal initial segment; CLuc, C-terminal luciferase fragment; DMEM, Dulbecco modified essential medium; DMSO, dimethylsulfoxide; FGF, fibroblast growth factor; FKBP, FK506-binding protein 12; FRB, rapamycin-binding domain; FRET, Forster (or fluorescence) resonance energy transfer; GFP, green fluorescent protein; iFGF, intracellular fibroblast growth factor; IκB, inhibitor of NFκB; IKK, IκB kinase; LCA, split-luciferase complementation assay; MAPK, mitogen-activated protein kinase; Nav channel, voltage-gated Na^+ channel; NFκB, nuclear factor κB; NLuc, N-terminal luciferase fragment; PBS, phosphate-buffered saline; PCR, polymerase chain reaction.

DOI: 10.1089/adt.2011.413

intracellular FGFs (iFGFs; FGF11–13), a group of molecules that remain intracellular, are not secreted, and exhibit selective tissue localization.[7] Through a high affinity monomeric interaction with the intracellular C-terminal tail of Nav channel α subunits (Nav1.1–Nav1.9), FGF14 acts as a multivalent molecule that controls neuronal excitability promoting gating, stability, and targeting of native Nav channels to the action potential initiation site.[8–13] Co-expression of neuronal FGF14 (FGF14-1b isoform) with different Nav channel isoforms results in modulation of Nav current amplitude and of voltage dependence of channel activation and inactivation of a magnitude and direction that depend upon the channel isoform and are distinct compared with any reported effects of other iFGFs on Nav channel function.[8–19] Furthermore, genetic deletion of *fgf14* in rodents impairs neuroplasticity and cognitive function, and single missense mutations of *FGF14* in humans results in neurodegeneration, highlighting the functional relevance of FGF14 as a critical component of the Nav channel macromolecular complex.[10,12,20–23] Although the structure of the FGF14:Nav channel complex, or of any other iFGF:Nav channel complexes, has not been resolved yet, information on critical residues of the iFGFs:Nav channel interface has been inferred from the FGF13 dimer crystal structure. The analysis of crystal packing contacts of the FGF13 dimer combined with mutagenesis experiments has demonstrated the existence of a conserved iFGF monomer interface that is proposed to mediate both homodimerization and Nav channel binding.[9] Point mutations of presumptive hot spots at this interface impair FGF13 regulation of Nav currents and disrupt subcellular targeting and co-localization of FGF14 with native Nav channels at the axonal initial segment (AIS).[9] Overall, the functional significance of FGF14 and the availability of structural information on the iFGFs:Nav channel complex makes the FGF14:Nav channel complex a potential target for proteomics-based discoveries and drug development directed toward regulation of Nav channel function and, ultimately, for treatment of disorders associated with dysregulation and/or mutations of Nav channels (epilepsy, neurodegeneration, pain, or other channelopathies).

As a first step in an FGF14-based medication development, we identified the need for simple and rapid methods for the detection and functional evaluation of protein–channel complexes that could rapidly translate into drug development campaigns targeting ion channels.

Traditional biochemical methods used for protein–protein interaction studies include enzyme-linked immunosorbent assays, surface plasmon resonance, and fluorescence polarization, while the functional effect of protein binding to ion channels has been studied using manual and/or automated patch-clamp electrophysiogy,[24] fluorescence-based methods,[25] or ion flux assays.[26] However, these assays are either relatively low throughput, not optimized for protein–channel complexes (electrophysiology), or costly and time demanding because they require the use of antibodies, high yield of purified proteins, or chemical derivation of the interacting protein pair. Conversely, split-protein reporters have emerged as a powerful methodology for the detection of biomolecular interactions in intact systems.[27] The concept behind this approach relies on the complementation of two separated halves of a monomeric enzyme driven by the assembly of two interacting partners. First utilized with ubiquitin,[28] the approach has been extended to dihydrofolate reductase,[29] β-lactamase,[30] GFP,[31,32] and various luciferase species, such as *Renilla* luciferase,[33] *Gaussia* luciferase,[34] and *Photinus* firefly luciferase.[35] The use of bioluminescence-based assays has become progressively more prominent in recent years.[36] High signal-to-noise ratio, favorable dynamic range, and reversibility of luminescence-based signals have revealed the split-luciferase complementation as a very sensitive assay to detect protein–protein interactions, protein localization, intracellular protein dynamics, and protein activity in real time and in living cells and animals.[35,37]

In the present study, we sought to assess the utility of the *Photinus* firefly split-luciferase complementation assay (LCA) for rapid evaluation of the FGF14:Nav1.6 channel C-tail complex in living cells. Toward this goal, we adapted and optimized the LCA to detect the FGF14:Nav1.6 channel C-tail complex assembly, and further employed the assay to identify critical amino acid residues responsible for the protein–channel interaction and to screen for upstream modulatory elements that alter complex formation. The data presented here support the use of the LCA as an innovative platform for rapid screening of protein–protein interactions within ion channel complexes.

MATERIALS AND METHODS

Chemicals

D-luciferin was purchased from Gold Biotechnology (St. Louis, MO) and prepared as a 30 mg/mL stock solution in phosphate-buffered saline (PBS); SP600125 (1,9-pyrazoloanthrone) was purchased from EMD Chemicals (San Diego, CA); PD169316 (4-(4-fluorophenyl)-2-(4-nitrophenyl)-5-(4-pyridyl)-1H-imidazole) was purchased from Sigma-Aldrich (St. Louis, MO); and BAY 11-7082 ((E)3-[(4-methylphenyl)sulfonyl]-2-propenenitrile) was purchased from Cayman Chemical (Ann Arbor, MI). The compounds were dissolved in dimethyl sulfoxide (DMSO).

DNA constructs

Mammalian expression vectors coding for N-terminal (pcDNA3.1-V5_HIS TOPO; rapamycin-binding domain [FRB]-N-terminal luciferase fragment [FRB-NLuc]) and C-terminal (pEF6-V5_HIS TOPO; C-terminal luciferase fragment [CLuc-FKBP]) fragments of firefly (*Photinus pyralis*) luciferase were a gift of Dr. Piwnica-Worms (Washington University, St. Louis, MO). To generate the CLuc-FGF14 construct, FKBP was replaced with neuronal FGF14 (1b isoform) in the CLuc-FKBP fusion vector. CLuc-FGF14 was engineered by polymerase chain reaction (PCR) amplification of the FGF14 open reading frame (nt 1–855) using a 5′ primer containing a *Bsi*WI site up to a linker region and a 3′ primer containing a *Not*I site and ligated into the CLuc vector. To generate the CD4-Nav1.6-NLuc construct, a chimera carrying the C-terminal fragment of Nav1.6 (amino acids 1763–1976) fused with CD4ΔCtail (amino acids 1–395; gift of Dr. Benedict Dargent, INSERM, France) was similarly replaced with FRB in the FRB-NLuc construct using PCR amplification and ligation into

*Bam*HI at the 5′ end and *Bsi*WI at the 3′ end. The choice of using the CD4 chimera fused to Nav1.6 C-tail was based on previous validations of this and other similar constructs in primary hippocampal neurons.[38–40] Because the N-terminus of the Nav channels is located intracellularly, the fusion of the NLuc fragment to the Nav1.6 C-tail resulted in intracellular reconstitution of the two halves of luciferase. The following primers were used for PCR amplification:

CLuc-FGF14:

Sense: 5′-CTCGTACGCGTCCCGGGGCGTAAAACCGGTGCCCCTCTTC-3′;

Antisense: 5′-GTTTAGCGGCCGCCTATGTTGTCTTACTCTTGTTGACTGG-3′.

CD4-Nav1.6-C-tail-NLuc:

Sense: 5′-CGGGGTACCCAAGCCCAGAGCCCTGCCATTTCTGTGGGCTCAGGT3′;

Antisense: 5′-CGCGTACGAGATCTGGCACTTGGACTCCCTGACCTCTTTTTGCCT-3′.

The FGF14$^{Y153N/V155N}$ mutant was engineered similarly to CLuc-FGF14 using pQBI-FGF14$^{Y158N/V160N}$–GFP as a template in the PCR reaction.[9,11] Note that the FGF14$^{Y153N/V155N}$ mutant presented in this study corresponds to the FGF14$^{Y158N/V160N}$ mutant described in previous studies.[9] All constructs were verified by DNA sequencing. The plasmid pGL3 expressing full length firefly luciferase, used for counter screenings of kinase inhibitors, was a gift of Dr. Sarkar (University of Texas Medical Branch [UTMB], Department of Neurology).

Cell culture and transient transfections

HEK293 cells were incubated at 37°C with 5% CO_2 in medium composed of equal volumes of Dulbecco modified essential medium (DMEM) and F12 (Invitrogen, Carlsbad, CA) supplemented with 10% fetal bovine serum, 100 U/mL penicillin, and 100 µg/mL streptomycin. For transfection cells were seeded in 24-well CELLSTAR® tissue culture plates (Greiner Bio-One, Monroe, NC) at 4.5×10^5 cells per well and incubated overnight to give monolayers at 90%–100% confluency. The cells were then transiently cotransfected with pairs of plasmids or single plasmids using Lipofectamine 2000 (Invitrogen), according to the manufacturer's instructions. Each plasmid used per transfection per well was 1 µg, unless otherwise indicated. Cells co-transfected with the CLuc-FGF14 and CD4-Nav1.6-C-tail-NLuc constructs (1 µg of each construct per transfection) were used as a positive control; cells co-transfected with CLuc-FGF14 and pcDNA3.1 empty vector (1 µg of each construct per transfection; this pair is referred to in the text as CLuc-FGF14 alone) were used as background luminescence. The same ratio and plasmid DNA amounts were used for the experiments involving the CLuc-FGF14$^{Y153N/V155N}$ and CD4-Nav1.6-C-tail-NLuc complex.

Bioluminescence assays

Forty-eight hours post-transfection, cells were trypsinized (0.25%) for 10 min at 37°C, triturated in a medium, and seeded in white, clear-bottom CELLSTAR µClear® 96-well tissue culture plates (Greiner Bio-One) at $\sim 10^5$ cells per well in 200 µL of medium. The cells were incubated for 24 h and then the growth medium was replaced with 100 µL of serum-free, phenol red–free DMEM/F12 medium (Invitrogen). In experiments involving protein kinase inhibitors compounds dissolved in DMSO (stock solution = 10 mM; intermediate dilutions = 0.2 mM, 0.5 mM, 1 mM, 2 mM, 4 mM, 6 mM, 8 mM in DMSO) were added to the final concentration of 1–50 µM in the culture medium; the final concentration of DMSO was maintained at 0.5% and positive control wells were also treated with 0.5% DMSO (treated positive control). Luminescence measurements were performed 1 h after the application of compounds. The reporter reaction was initiated by injection of 100 µL of substrate solution containing 1.5 mg/mL of D-luciferin (final concentration = 0.75 mg/mL) dissolved in serum-free, phenol red–free DMEM/F12 medium. Dispensing of the substrate was performed by the Synergy™ H4 Multi-Mode Microplate Reader (BioTek, Winooski, VT). Luminescence readings were initiated after 3 s of mild plate shaking and performed at 2-min intervals for 20 min, integration time 0.5 s. The cells were maintained at 37°C throughout the measurements. Signal intensity for each well was calculated as a mean value of peak luminescence and luminescence measured at two adjacent time points; the calculated values were expressed as percentage of mean signal intensity in the control samples from the same experimental plate.

Molecular modeling

The PDB coordinates for the FGF14 model based on the FGF9 crystal structure were generously provided by Dr. Van Swieten (Department of Neurology, Erasmus Medical Center, Rotterdam). This FGF14 homology model[21] was used as a template. The electrostatic surface representation and FGF14$^{Y153N/V155N}$ mutations were carried out *in silico* within the University of California San Francisco (USCF) Chimera suite[41] applying the Richardson rotamers algorithm.[42]

Measurement of cell viability

The number of viable transfected cells after treatment was estimated by CyQUANT® Cell Proliferation Assay Kit (Invitrogen) according to manufacturer's instructions after incubation with 0.5% DMSO or appropriate kinase inhibitors. Fluorescence was measured using the Synergy™ H4 Multi-Mode Microplate Reader (excitation $\lambda = 485$ nm, emission $\lambda = 528$ nm). Cell viability was expressed as percent mean fluorescent signal intensity in the control samples from the same experimental plate.

Data analysis

Statistical values are given as mean and standard error of the mean (mean ± SEM), unless otherwise specified. The following control groups were used: (i) CLuc-FGF14 + CD4Nav1.6-NLuc, untreated (untreated positive control); (ii) CLuc-FGF14 + CD4Nav1.6-NLuc, treated with 0.5% DMSO (treated positive control); (iii) CLuc-FGF14 alone, untreated (reference background); (iv) CLuc-FGF14 + CD4Nav1.6-NLuc treated with 50 µM BAY 11-7082 (negative control and background). In the experiments involving the FGF14$^{Y153N/V155N}$ mutant, untreated control was used for comparison. Initial

experiments were performed to evaluate the sensitivity of the assay to 0.5% DMSO by comparing untreated positive controls to treated positive controls ($n=4$, t-test, $p=0.262$). In the experiments evaluating the effect of kinase inhibitors DMSO treated controls were used for comparison.

Statistical parameters of assay performance were calculated according to the following formulas:

$$Z'\text{ factor} = 1 - 3\times(\delta_p + \delta_n)/(\mu_p - \mu_n) \quad (1)$$

$$S:B = \mu_p/\mu_n \quad (2)$$

$$S:N = (\mu_p - \mu_n)/\sqrt{\sigma_p^2 + \sigma_n^2} \quad (3)$$

$$SW = [\mu_p - \mu_n - 3\times(\sigma_p + \sigma_n)]/\sigma_p \quad (4)$$

where δ_p and δ_n are standard deviation of the positive group p and the negative control group n, and μ_p and μ_n are the mathematical means of the two groups, respectively; S:B, signal to background; S:N, signal-to-noise; and SW, signal window. The positive control group for assay performance evaluation was CLuc-FGF14 + CD4Nav1.6-NLuc treated with 0.5% DMSO and the negative control was CLuc-FGF14 + CD4Nav1.6-NLuc treated with 50 μM BAY 11-7082.

Dose–response curves and IC_{50} for each compound were obtained by fitting the data with a nonlinear regression:

$$y = A_1 + [A_2 - A_1/1 + 10^{\log_{10}(x_0 - x)^p}] \quad (5)$$

where x is $\log_{10}$ of the compound concentration in M, x_0 is the inflection point (IC_{50}), A_1 is the initial strength, A_2 is the offset, and p is the Hill slope.

The adjusted coefficient of determination between number of plated cells or amount of transfected cDNA plasmid and luminescence signal (*Supplementary Fig. S1*; Supplementary Data are available online at www.liebertonline.com/adt) was determined using the following equation:

$$R^2_{adj} = 1 - (RSS/df_{error})/(TSS/df_{total}) \quad (6)$$

where RSS is residual sum of square, TSS is total sum of square, df total is the degrees of freedom $n-1$ of the estimate of the population variance of the dependent variable, and df_{error} is the degrees of freedom $n-p-1$ of the estimate of the underlying population error variance.

The statistical significance ($p<0.05$) of observed differences among groups was determined by Student's t-test, one-way ANOVA with *post hoc* Dunnett's, Kruskal–Wallis one-way ANOVA on ranks with *post hoc* Dunn's method, or ANOVA using Sigma Stat software (Jandel Inc., San Jose, CA). The ANOVA values were not statistically different from each other and no *post hoc* analysis was required. The choice of ANOVA (parametric) versus Kruskal–Wallis (nonparametric) tests was based on normality and equal variance analysis performed with Sigma Stat. Fitting and graphs were generated in Origin Software (Origin Lab Corporation, Northampton, MA).

Western blotting

Transfected HEK293 cells treated with compounds were washed with PBS and lysed in buffer containing 20 mM Tris-HCl, 150 mM NaCl, and 1% NP-40. Protease inhibitor cocktail (set 3, Calbiochem, La Jolla, CA) was added immediately before cell lysis. Cell extracts were collected, sonicated for 20 s, and centrifuged at 4°C, 15,000 *g* for 15 min adding 2× sample buffer containing 50 mM tris(2-carboxyethyl)phosphine. Mixtures were heated for 10 min at 65°C and resolved on 4%–15% polyacrylamide gels (BioRad, Hercules, CA). Resolved proteins were transferred to PVDF membranes (Millipore, Bedford, MA) for 1.5 h at 4°C and blocked in tris-buffered saline with 3% nonfat dry milk and 0.1% Tween-20. Membranes were then incubated overnight in blocking buffer containing the anti-luciferase goat polyclonal antibody (Promega, Madison, WI) or anti-calnexin rabbit polyclonal antibody (Cell Signaling Technology, Danvers, MA). Washed membranes were incubated with donkey anti-goat or goat anti-rabbit-horseradish peroxidase (1:5000) and visualized with ECL Advance Western Blotting Detection kit (GE Healthcare, Piscataway, NJ); protein bands were visualized using FluorChem® HD2 System and analyzed with AlphaView 3.1 software (ProteinSimple, Santa Clara, CA).

RESULTS

LCA detection of the FGF14:Nav channel C-tail complex

To develop reliable methods to study protein–channel complexes, we initially set out to determine whether the FGF14:Nav channel C-tail complex assembly was detectable in live cells. We adapted the LCA to detect the assembly of FGF14 and the C-terminus tail of the Nav1.6 channel in HEK293 cells. In this assay, two constructs bearing the complementary N-terminus (NLuc) and C-terminus (CLuc) fragments of the firefly luciferase[35] were fused, respectively, to a chimera of the CD4 transmembrane segment and the C-tail of Nav1.6[38] (CD4-Nav1.6-NLuc) or FGF14 (CLuc-FGF14) (*Fig. 1A*) and transiently expressed in HEK293 cells, following a 3-day experimental scheme (*Table 1*). Co-transfection of CD4-Nav1.6-NLuc and CLuc-FGF14 constructs in HEK293 cells led to ~50-fold increase in the luminescence signal generated after addition of the substrate, D-luciferin (*Fig. 1B*), compared to background (CLuc-FGF14 alone, *Fig. 1C*). The luminescence signal reached a steady-state maximal value after 12–15 min that persisted to the end of each experiment (20–30 min), indicating a robust assembly of the FGF14:Nav1.6 complex in live cells. Optimal amounts of transfected plasmid DNA and number of transfected cells seeded per well prior to luminescence measurements were determined as part of the assay development effort (*Table 1, Supplementary Fig. S1*). The level of luminescence correlated with the amount of transfected plasmid DNA ($R^2=0.96$) and the number of cells plated ($R^2=0.99$). A total of 2 μg of DNA (1 μg per construct) and a cell seeding density of 1.5×10^5 cells/well (96-well plate) produced the strongest luminescence signal (*Supplementary Fig. S1*). Increasing the total amount of transfected DNA above 2 μg resulted in lower luminescence signal (data not shown), presumably due to cell toxicity. Based on these results, we concluded that LCA is a useful

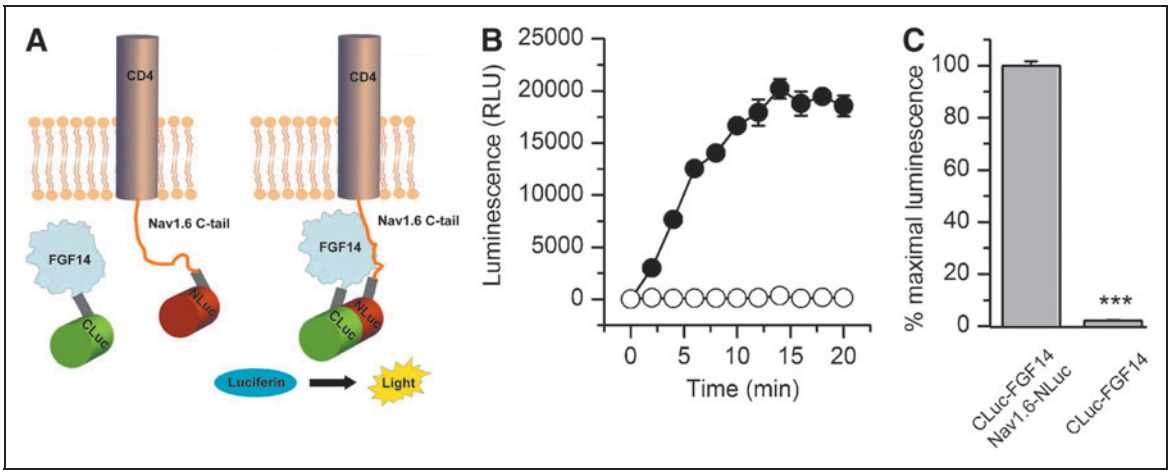

Fig. 1. Bioluminescence detection of the FGF14:Nav1.6 C-tail complex in live cells using the split-luciferase complementation assay. **(A)** Schematic of the split-luciferase complementation assay (LCA). Constructs expressing the CLuc (398–550) and NLuc (2-415) fragments of firefly *Photinus pyralis* luciferase were fused, respectively, to full-length FGF14 and a chimera of the transmembrane protein CD4 and the C-terminal tail of Nav1.6. A flexible linker (gray) spaces the FGF14 and CD4-Nav1.6 cDNA from the two halves of luciferase. Spontaneous association of FGF14 and Nav1.6 C-tail brings in close proximity the two halves of luciferase leading to recombination of the luciferase enzymatic activity and luminescence production in the presence of the substrate D-luciferin (right). **(B)** HEK293 cells were transiently transfected with either CLuc-FGF14 or CD4-Nav1.6-NLuc (●) or CLuc-FGF14 alone (○). The assembly of the FGF14:Nav1.6 channel C-tail complex is detected as luminescence (relative luminescence units, RLU) upon the addition of the D-luciferin (0.75 mg/mL) substrate at time zero; data are mean ± SEM from quadruplicate wells from one single experiment. **(C)** Bar graph represents % maximal bioluminescence measured upon functional complementation of the indicated constructs. The CLuc-FGF14 + CD4-Nav1.6-NLuc pair represents the positive control, whereas CLuc-FGF14 alone serves as reference luminescence background. The data are mean ± SEM representing eighth replicates from four independent experiments (CLuc-FGF14 + CD4-Nav1.6-NLuc, $n = 4$) or four replicates from three independent experiments (CLuc-FGF14 alone, $n = 3$). The background level was 2.1 ± 0.25% compared to the positive control. The signal-to-background level was 81 ± 4.2. The mean values are compared using Student's *t*-test; ***$p < 0.001$.

Table 1. Bioluminescence Assay Protocol

Step	Parameter	Value	Description
1	Transfect cells	50 µL/well	80% confluent HEK293 cells
2	Incubation time	48 h	Cell growth and plasmid expression
3	Replate cells	24 h	1.5×10^5 cells/well (1:4 dilution from step 2)
4	Compounds and controls	0.5 µL/well	1–50 µM (test compounds) 0.5% DMSO in 100 µL of serum-free, phenol red–free medium
5	Compound incubation	1 h	Compound equilibrium
6	Luciferase substrate loading	D-luciferin (final concentration = 0.75 mg/mL)	Luciferase enzymatic activity
7	Assay readout	PMT sensitivity = 254; 560 nm	Relative luminescence units

Step Notes
1. Greiner white-walled 24-well plate.
2. 37°C and 5% CO_2.
3. Greiner white-walled 96-well plate.
4. Stock concentration of compounds is 0.2–10 mM; 0.5% DMSO control.
5. 37°C and 5% CO_2.
6. Detection of complementation of the luminescent protein pairs.
7. Synergy H4 Multi-Mode Microplate Reader; integration time 0.5 s.

PMT, photomultiplier tube.

tool for rapid evaluation of ion channel macromolecular complexes in live cells.

LCA validation of protein–channel interface hot spots

To evaluate whether LCA would be suitable for in-cell validation of hot spots at protein–channel interfaces, we showed *in silico* mutations of critical residues at the predicted FGF14:Nav channel interface. FGF14 and other iFGFs bind to the Nav channel C-tails as monomers and this homodimerization interface is also responsible for Nav channel binding.[9] Residues Y153 and V155 in FGF14 and the corresponding residues in all iFGFs have been shown to be critical for Nav channel binding.[9] Thus, we posited that that these residues could be hot spots at the

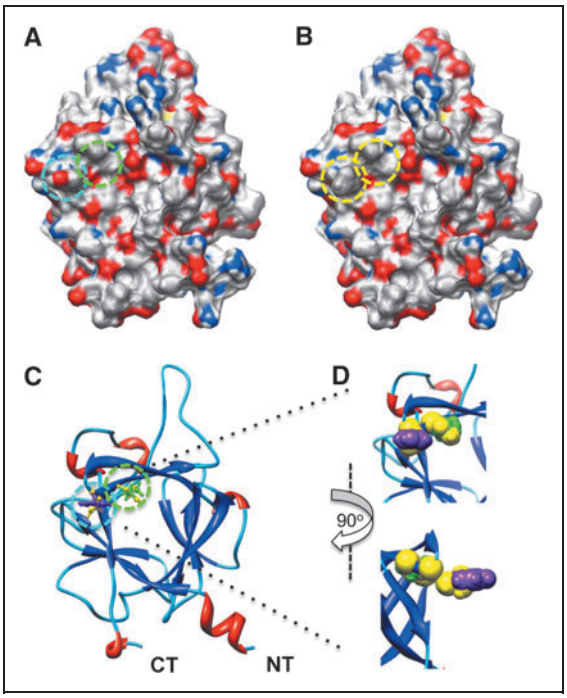

Fig. 2. *In silico* model of the FGF14$^{Y153N/V155N}$ mutations. Electrostatic surface representation of FGF14 wild type **(A)** and FGF14$^{Y153N/V155N}$ double mutant **(B)**. The positive charged surfaces are in blue and the negative charged surfaces in red. In **(A)**, the cyan dashed circle denotes the surface corresponding to the Y153 and the green dashed circle to the V155. In **(B)**, the yellow dashed circles denote the surfaces corresponding to the N153 and N155 in the Y153N/Y155N mutant. **(C)** Ribbon representation of the secondary structures of overlapped FGF14 wild type and FGF14$^{Y153N/V155N}$ mutant. The αC backbone of the α-helices in red, the β-strand in blue, and the random structures in light blue are shown as ribbons. The C-terminal and N-terminal tails are denoted as CT and NT, respectively. The side chains corresponding to the Y153 (purple) and V155 (green) in the FGF14 wild type, and the side chains corresponding to the N153 and N155 (yellow) in the FGF14$^{Y153N/V155N}$ double mutant are superimposed on the FGF14 wild-type structure and are shown as ball and sticks. **(D)** Magnified orthogonal views of Y153 (purple), V155 (green), and N153 and N155 (yellow) side chains from **(C)** are shown as spheres.

FGF14:Nav channel interface. To visualize the effect of the previously studied FGF14$^{Y153N/V155N}$ double mutation[9] at the potential FGF14:Nav channel interface, we carried out *in silico* the Y153N and V155N mutations (*Fig. 2*). Mutating Tyr153 to Asn reduces the net negative charge due to the OH group from the Tyr side chain (*Fig. 2A, B*), additionally modifying the β8-β9 loop surface due to the replacement of the cyclic bulky Tyr ring with the less bulky Asn side chain (*Fig. 2D*). Mutating the Val155 to Asn modifies further the cavity adjacent to Tyr153 (*Fig. 2D*). Simultaneously mutating Tyr153 and Val155 to Asn reduces the overall negative charge and smoothes the predicted FGF14:Nav channel interface at the level of the β8-β9 strands loop, where Tyr153 and Val155 are positioned. We utilized the LCA to determine whether these predicted structural alterations in the channel-binding interface would result in decreased assembly of the FGF14:Nav1.6 complex. The complementation of the FGF14$^{Y153N/V155N}$:Nav1.6 complex was measured over time (*Fig. 3A*) and was significantly reduced in comparison to the wild type complex (*Fig. 3B*, 48.3 ± 3%, $n = 4$, Student's *t*-test, $p < 0.001$). However, since mutations are known to induce protein misfolding and degradation,[43] it was necessary to rule out changes in the protein expression level induced by the Y153N/V155N mutations as a mechanism for the reduced assembly of the mutated complex. To this end, we performed additional control experiments in which expression of CLuc-FGF14 and CLuc-FGF14$^{Y153N/V155N}$ was confirmed by Western blot analysis (*Fig. 3C*). The expression level of FGF14$^{Y153N/V155N}$ was comparable to FGF14 wild type, regardless of the presence or absence of CD4-Nav1.6-NLuc (*Fig. 3C, D*). Furthermore, FGF14$^{Y153N/V155N}$ did not significantly affect the expression level of CD-Nav1.6-NLuc (108 ± 13% compared to CD-Nav1.6-Nluc + FGF14 wild type, $n = 3$, paired *t*-test, $p = 0.49$). These results confirm that the nonproductive assembly of the FGF14$^{Y153N/V155N}$:Nav1.6 channel C-tail was not attributable to significant differences in the protein expression levels, but was rather consistent with structural changes at the level of the protein–protein interaction interface.

In-cell dynamic regulation of the FGF14:Nav1.6 C-tail complex

Having established that the LCA provides a rapid method for in-cell evaluation of critical residues at protein–protein interfaces, we next explored the dynamic regulation of the FGF14:Nav1.6 C-tail complex by intracellular signaling pathways, focusing on the role of kinases. Kinases are key regulators of neuronal excitability,[44,45] and phosphorylation is a posttranslational modification well known to affect macromolecular complexes. In the brain Nav channels are phosphorylated at multiple intracellular sites,[44,46] and these posttranslational modifications result in modulation of channel gating and trafficking with effects on neuronal excitability.[47] Interestingly, FGF14 sequence motif analysis (http://elm.eu.org; www.cbs.dtu.dk/services/NetPhos) identifies a plethora of putative, yet uncharacterized, phosphorylation sites either at the predicted FGF14:Nav channel interface or at influential modulatory sites in the FGF14 C-terminal tail.[9] However, the mechanism by which phosphorylation of Nav channels and FGF14 regulate reciprocal binding remains unknown. We posited that specific kinases could act on the FGF14:Nav1.6 complex assembly and be part of a phosphoproteome that could potentially control neuronal excitability through protein–protein interaction.

To test this hypothesis, we evaluated the effect of selective kinase inhibitors on the FGF14:Nav1.6 channel C-tail complex assembly. We chose chemical inhibitors of the mitogen-activated protein kinase (MAPK) p38 and the IκB kinase (IKK), a repressor of the nuclear factor κB (NFκB). Both MAPK/p38 and IKK have been directly or indirectly linked to iFGFs. In earlier studies, FGF12 was identified as a binding partner of islet brain 2 (IB2/JIP2), a scaffold protein of MAPKp38δ,[46] and IKK has been recently found at the AIS in a complex with

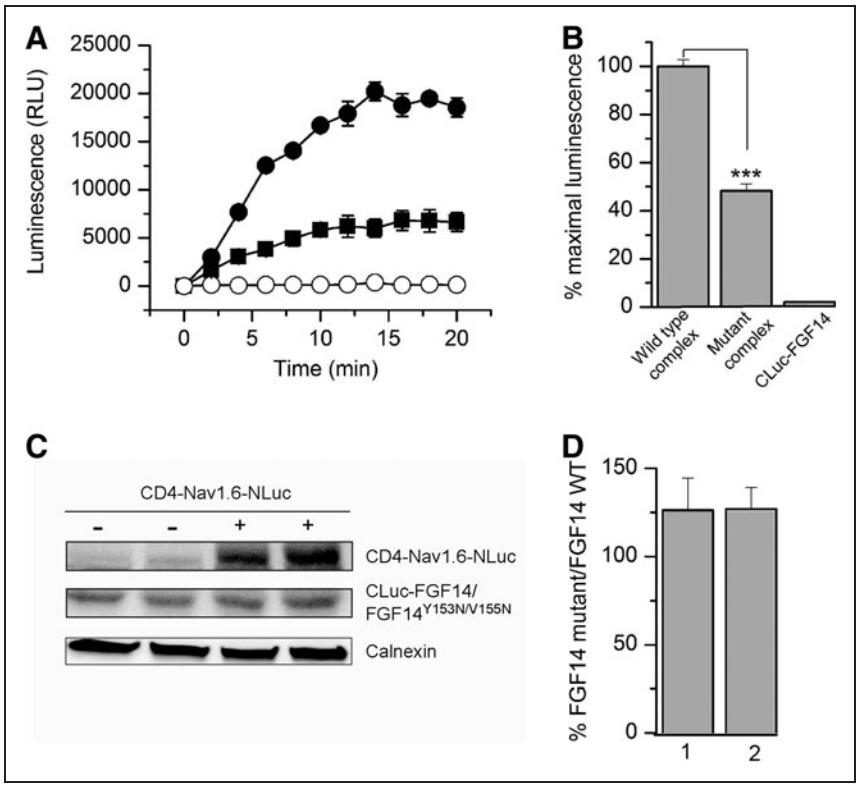

Fig. 3. LCA validates *in silico* predictions of the structure-function studies. **(A)** HEK293 cells were transiently transfected with CLuc-FGF14 and CD4-Nav1.6-NLuc (●), CLuc-FGF14$^{Y153N/V155N}$ + CD4-Nav1.6-NLuc (■) or CLuc-FGF14 alone (○). Assembly of the indicated pairs is detected as luminescence (relative luminescence units, RLU) upon the addition of the D-luciferin substrate at time zero. **(B)** Bar graph represents percent of maximal bioluminescence (normalized to wild-type control) measured upon complementation of the indicated constructs. The FGF14$^{Y153N/V155N}$ double mutant shows a reduced assembly with the Nav1.6 channel C-tail; data are mean ± SEM. The CLuc-FGF14 + CD4-Nav1.6-NLuc and CLuc-FGF14$^{Y153N/V155N}$ + CD4-Nav1.6-NLuc experimental groups consisted of eight replicates from four independent experiments; the statistical significance between the two groups was assessed using Student's *t*-test, $n = 4$, ***$p < 0.001$. CLuc-FGF14 alone represents reference luminescence background. **(C)** Western blots of whole-cell extracts (equal amount of protein per lane) from cells transfected with CLuc-FGF14 wild type (lane 1, from left), CLuc-FGF14$^{Y153N/V155N}$ (lane 2), CLuc-FGF14 + CD4-Nav1.6-NLuc (lane 3), and CLuc-FGF14$^{Y153N/V155N}$ + CD4-Nav1.6-NLuc (lane 4). Western blots were probed with a polyclonal anti-luciferase antibody. The anti-luciferase antibody recognizes different epitopes on the NLuc and CLuc fragments; immunodetection of calnexin is used as loading control. **(D)** Densitometry analysis of CLuc-FGF14$^{Y153N/V155N}$ (FGF14 mutant) normalized to CLuc-FGF14 (FGF14 WT) in the absence (1) or presence of CD4-Nav1.6-NLuc (2). The expression level of CLuc-FGF14$^{Y153N/V155N}$ was comparable to control in both conditions ($n = 4$, *t*-test, $p = 0.63$ for condition 1; $n = 4$, *t*-test, $p = 0.67$ for condition 2). Data are mean ± SEM.

iFGFs.[48] To determine the role of these kinases in modulating the FGF14:Nav1.6 channel C-tail complex assembly, HEK293 cells, co-transfected with CLuc-FGF14 and CD4-Nav1.6C-tail-NLuc, were exposed to the MAPKp38 inhibitor PD169316, the IKK inhibitor BAY 11-7082, the c-JNK (c-JNK terminal kinases) inhibitor SP600125, or vehicle (0.5% DMSO) for 1 h prior to the assay. The c-JNK cascade is another branch of the MAPK pathway,[49] and SP600125 was used as an internal control for specificity. Upon substrate addition, luminescence from various experimental groups was measured up to 20 min (*Fig. 4A*). Compared to DMSO, treatment with PD169316 or BAY 11-7082 significantly reduced the FGF14:Nav1.6 assembly to 54 ± 7.7% ($n = 3$, $p < 0.01$) and 52 ± 3.5% ($n = 3$, $p < 0.001$), respectively, while no significant changes in luminescence were observed upon SP00125 treatment (104 ± 6.6%, $n = 3$, $p = 0.53$, *Fig. 4B*). These data suggest that activation of the MAPKp38 and the IκB/NFκB pathways *in vivo* might promote assembly and stability of the FGF14:Nav channel complex. Whether these effects result from a direct phosphorylation of the complex remains to be determined.

Reports indicate chemical interference of compounds with the enzymatic activity of various species of luciferase.[50,51] To rule out that the observed results were induced by the effect of the compounds on the enzymatic activity of luciferase, the kinase inhibitors were screened against HEK293 cells transfected with full length firefly luciferase. Cells were exposed to either PD169316 (10 μM), BAY 11-7082 (10 μM), SP600125 (50 μM), or DMSO for 1 h; none of these compounds had a significant effect on firefly luciferase activity compared to DMSO-treated controls (*Fig. 4C*; PD169316, 86 ± 5%, $p = 0.11$; BAY 11-7082, 95 ± 9%, $p = 0.64$; SP600125, 112 ± 6.2%, $p = 0.21$; for all groups $n = 3$). Furthermore, we performed additional control experiments to rule out other potential artifacts including reduced cell viability or altered expression levels of the split constructs. Cell viability across experimental conditions was determined by the CyQuant fluorescence-based proliferation assay, and revealed no significant differences across conditions (*Fig. 4D*; PD169316, 78 ± 11%, $p = 0.14$; BAY 11-7082, 109.7 ± 9.7%, $p = 0.42$; SP600125 99.6 ± 13.9%, $p = 0.98$; for all groups $n = 3$). Western blot analysis confirmed that the CD4-Nav1.6-NLuc and CLuc-FGF14 expression levels were not affected by treatments with PD169316 (10 μM), BAY 11-7082 (10 μM), or SP600125 (50 μM) compared to DMSO-treated control cells (*Fig. 5*). Overall, these results indicate that the FGF14:Nav1.6 channel C-tail assembly is controlled by the activity of specific kinases. This mechanism might contribute to a complex, yet unknown, regulation of neuronal excitability through protein–protein interaction and provide a platform to develop chemical interventions against Nav channel–related diseases based on phosphoproteomic networks.

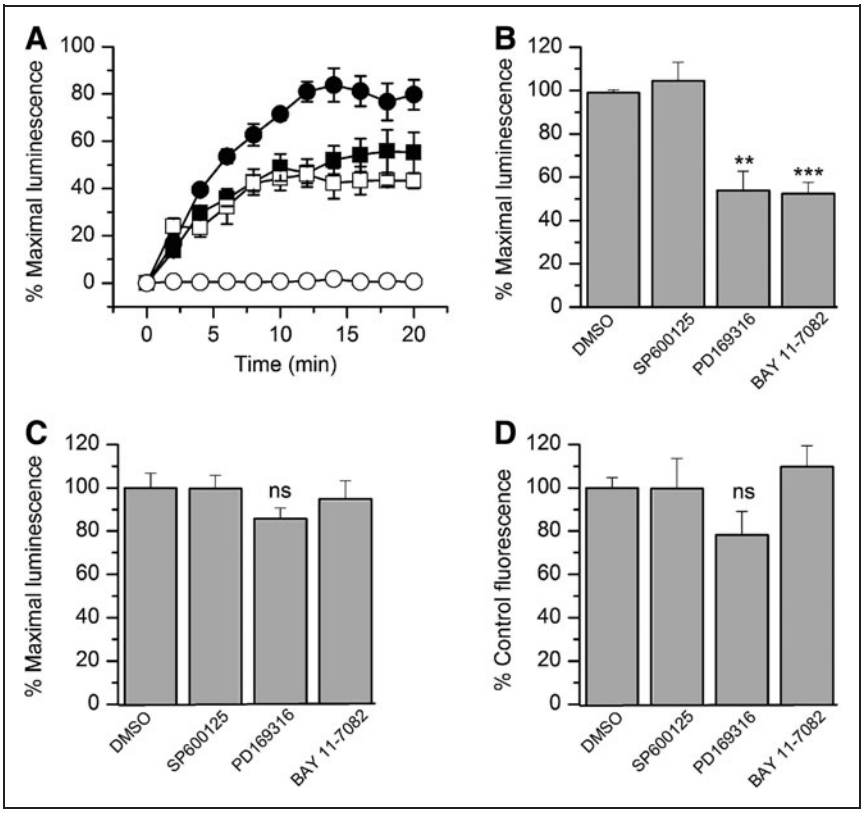

Fig. 4. The FGF14:Nav1.6 functional complementation is regulated by specific kinase inhibitors. **(A)** HEK293 cells were transiently transfected with CLuc-FGF14 and CD4-Nav1.6-NLuc and treated with the p38 kinase inhibitor PD169316 (10 μM; ■), the IKK inhibitor, BAY 11-7082 (10 μM; □) or dimethylsulfoxide (DMSO; 0.5% control; ●). Cells transfected with CLuc-FGF14 alone (○) are also shown. Assembly of the LCA pair is detected as luminescence upon the addition of the D-luciferin substrate at time zero and normalized to % maximal luminescence signal in DMSO (0.5%, control); data are mean ± SEM, representing quadruplicates from one representative experiment. **(B)** Bar graph represents mean ± SEM expressed as % maximal luminescence of control (0.5% DMSO). The graphs illustrates the effect of the c-JNK inhibitor SP600125 (50 μM), the p38 kinase inhibitor PD169316 (10 μM), and the IKK inhibitor BAY 11-7082 (10 μM) on the FGF14:Nav1.6 channel C-tail assembly. The control and the SP600125 and PD169316 experimental groups each consisted of four replicates from four independent experiments ($n = 4$); the BAY 11-7082 experimental group consisted of four replicates from three independent experiments ($n = 3$). Statistical significance between the four groups was assessed using one-way ANOVA, *post hoc* Dunnett's method, $^{**}p < 0.01$, $^{***}p < 0.001$. **(C)** HEK293 cells were transiently transfected with full-length firefly luciferase holoenzyme and treated for 1 h prior to the assay with the indicated compounds. Bar graph expressed as % maximal luminescence illustrates the effect of indicated compounds on the intrinsic enzymatic activity of luciferase; data are mean ± SEM representing four replicates from three independent experiments ($n = 3$). Statistical significance between the four groups was assessed using Kruskal–Wallis one-way ANOVA on ranks, *post hoc* Dunn's method; ns = nonsignificant. **(D)** HEK293 cells were transiently transfected with CLuc-FGF14 and CD4-Nav1.6-NLuc and treated with the indicated compounds. The effect of compounds on cell viability was determined by using CyQUANT® Cell Proliferation Assay Kit. Bar graph expressed as % control fluorescence illustrates the effect of the indicated compounds on cell viability. Data are mean ± SEM, $n = 3$. Statistical significance between the four groups was assessed using one-way ANOVA; ns = nonsignificant. None of the treatments in **(D)** were significantly different from each others, and no further *post hoc* analysis was required.

In-cell dose responses using LCA

Finally, we determined the use of the LCA as a rapid tool for in-cell pharmacology. HEK293 cells transiently transfected with CLuc-FGF14 + CD4Nav1.6-NLuc were exposed to a range of concentrations (1–50 μM) of either PD169316 or BAY 11-7082, or to DMSO (0.5%) for 1 h; maximal luminescence for each experimental group was used to construct dose–response curves. Fitting with nonlinear regression yielded comparable IC_{50} values of 8.9 ± 0.93 μM and 8.8 ± 0.85 μM for PD169316 and BAY 11-7082, respectively (*Fig. 6*). Notably, the IC_{50} values of both kinase inhibitors were consistent with those reported in other in-cell studies.[52,53] In an effort to evaluate assay reproducibility, Z′-factor, signal-to-background, signal-to-noise ratio, and signal window[37,54,55] were determined by comparing luminescence values in CLuc-FGF14 + CD4Nav1.6-NLuc cells treated with 0.5% DMSO (positive control) versus BAY 11-7082 (50 μM; negative control and/or background), as illustrated in *Figure 7*. Exposure of cells to 50 μM BAY 11-7082 did not affect cell viability (132.4 ± 18.3% compared to DMSO control, $n = 3$, *t*-test, $p = 0.25$). Overall, these results indicate that upon optimization to 384- or 1536-well plate format LCA would be valuable for rapid evaluation of compound potency in cells and might be used to expedite hit validation in high-throughput screening campaigns.

DISCUSSION

In the studies described here we demonstrate for the first time the use of the LCA as a rapid assay to detect the assembly of the FGF14:Nav1.6 channel C-tail complex, to validate hot spots at this protein–protein interaction complex and to investigate its dynamic regulation by kinases in live cells. We chose to focus on this protein complex for the following reasons. First, neuronal FGF14 is a functionally relevant component of the Nav channelosome that controls Nav channel gating properties and expression with a complexity and potency unique to any other iFGFs or other known Nav interactors.[8–13] Furthermore, in rodents genetic deletion of *fgf14* impairs neuroplasticity and cognitive function, and in humans mutations of *FGF14* result in neurodegeneration,[20,21] indicating an important preclinical and translational significance to this brain molecule.[10,12,22,23,56] Of all Nav channel α subunits detected in complex with FGF14, Nav1.6 was chosen because it is the most sensitive to FGF14 modulation.[8] Nav1.6

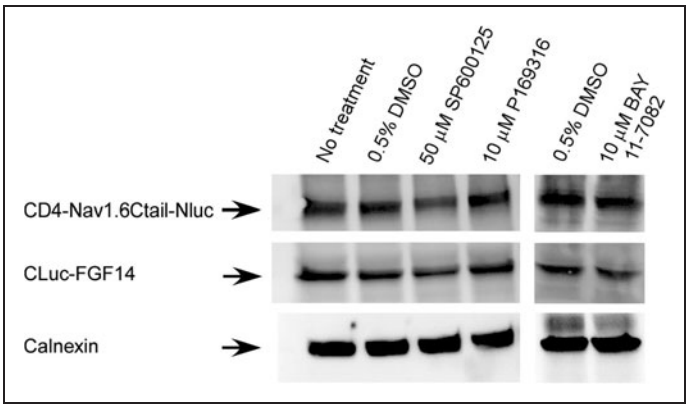

Fig. 5. Effect of kinase inhibitors on protein expression levels. Representative example of Western blots of whole-cell extracts (equal amount of protein per lane) from cells transfected with CLuc-FGF14 + CD4-Nav1.6-NLuc and treated for 1 h with the indicated compounds (total number of experiments = 3). Western blots were probed with a polyclonal anti-luciferase antibody; immunodetection of calnexin is used as loading control.

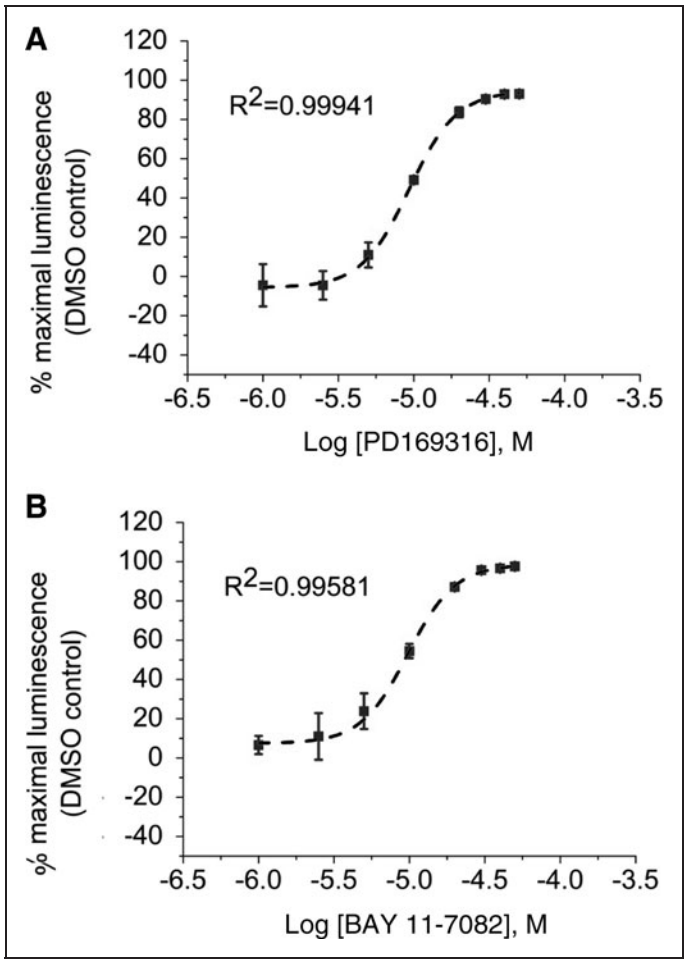

Fig. 6. Evaluation of the potency of selective kinase inhibitors. HEK293 cells were transiently transfected with CLuc-FGF14 and CD4-Nav1.6-NLuc and treated with the indicated concentrations of PD169316 **(A)** or BAY 11-7082 **(B)**. Dose–response inhibition of the FGF14:Nav1.6 channel C-tail assembly upon treatment with PD169316 (four replicates from one experiment) and BAY 11-7082 (eight replicates from two independent experiments); data are mean ± SEM. The IC_{50} calculated by fitting the nonlinear regression equation (dotted line) is 8.9 ± 0.93 μM (PD169316) and 8.8 ± 0.85 μM (BAY 11-7082).

channels play a critical role in fine tuning neuronal excitability,[57] are linked to human diseases,[58,59] and pharmacological inhibition of Nav1.6 channels is neuroprotective.[60] Thus, the development of this new assay to detect the FGF14:Nav1.6 channel C-tail complex and to rapidly screen its dynamic modulation could provide a launching platform for probe development and drug discovery in the central nervous system.

The bioluminescence-based LCA introduced by Luker *et al.*[35] provides a quantitative and reversible real-time readout of protein–protein interactions *in vitro* and *in vivo* and is an emerging alternative to fluorescence-based assays (for example, FRET[25]). In our adaptation of this assay, the two complementary N-terminus (NLuc 2-416) and C-terminus (CLuc 398-550) fragments of firefly luciferase were, respectively, fused into a chimera of the CD4 transmembrane segment and the Nav1.6 C-tail (CD4-Nav1.6-NLuc) or human FGF141b isoform (CLuc-FGF14). The use of a construct expressing solely the Nav1.6 C-tail presents several advantages: (i) it is an alternative to the expression of full-length recombinant Nav channels, which are high molecular weight transmembrane proteins hard to express into heterologous expression systems; (ii) it preserves the Nav channel C-tail natural orientation juxtaposed to the plasmamembrane and its membrane targeting;[39] (iii) it isolates the C-tail from the rest of the Nav channel, limiting any potential indirect modulatory effects on the protein–channel complex induced by other intracellular domains of Nav. However, future optimizations might include the development of stable cell lines expressing full-length Nav channel constructs tagged to one of the luciferase fragments (either N- or CLuc) for use in simultaneous LCA and automated-patch clamp or fluorescence-dye platforms. Co-transfection of CD4-Nav1.6-NLuc and CLuc-FGF14 constructs in HEK293 cells resulted in a robust and stable assembly of the protein–channel C-tail complex over time. Z′ factor, signal-to-background, and signal-to-noise values[37,54] were in agreement with previous in-cell luminescence complementation assays.[61,62] Thus, upon miniaturization and up-scaling from 96-well to 1536-well plates format, we envision that this assay will be suitable for large high-throughput screening.

We have explored the use of the LCA for validating structural changes at the FGF14:Nav1.6 channel complex interface. Our results show that residues Y153 and V155 play a critical role in the interaction with Nav1.6, and in agreement with previous studies,[9] we confirm by *in silico* analysis of the Y153N/V155N mutations that these residues are part of a hot spot at the FGF14:Nav1.6 channel interface. When evaluated in the LCA, mutations of Y153 and V155

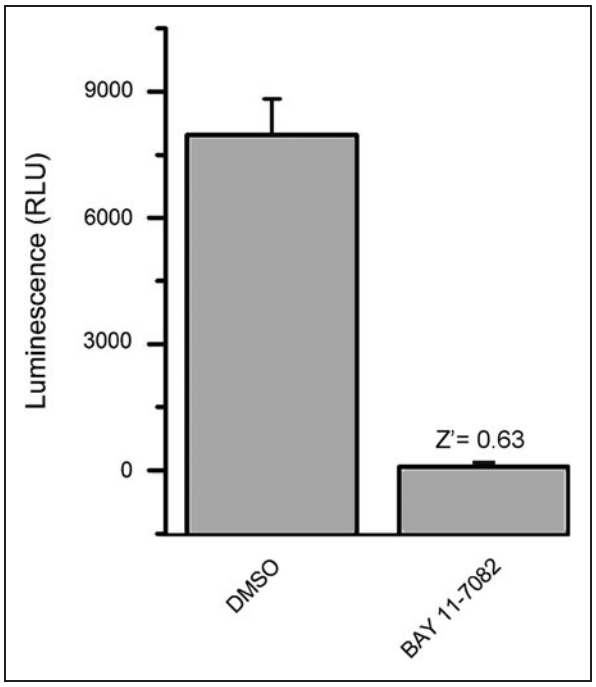

Fig. 7. Evaluation of assay reliability. Luminescence values from HEK293 cells transiently transfected with CLuc-FGF14 + CD4-Nav1.6-NLuc and either treated with 0.5% DMSO (positive control) or BAY 11-7082 (negative control and/or background) were 7970 ± 150 RLU and 84.2 ± 4.5 RLU, respectively. Signal-to-noise ratio was 142, signal-to-background was 95.3, and signal window was 5.3. Data are mean ± SD; the statistical parameters were calculated over $n = 32$ wells for each group.

into N led to a reduction of the FGF14:Nav1.6 assembly, with no effects on FGF14 expression levels, confirming our hypothesis that these residues are likely to impose structural changes at the protein–complex interface. Evaluation of additional residues identified *in silico* will be necessary, however, to fully characterize the structure and specificity of the FGF14:Nav1.6 channel interface. The effect of naturally occurring mutations of either FGF14 ($FGF14^{F145S}$, SCA27 mutant[21]) or of the Nav channel C-tail on reciprocal interactions are also important and could be evaluated using the LCA. Interestingly, the folding-defective Nav1.1-M1841T epileptogenic mutant can be partially rescued by co-expression with the β1 accessory subunit, raising the possibility of utilizing protein–protein interactions as a base for medication development against channelopathies.[63–65] Thus, the LCA not only provides a useful tool for rapid screenings of hot spots at relevant protein–channel interfaces, but it might also be useful to evaluate the impact of disease-linked mutations on the assembly of macromolecular complexes.

We have also explored the dynamic regulation of the FGF14:Nav1.6 complex by intracellular signaling pathways by evaluating the effect of selective kinase inhibitors on the FGF14:Nav1.6 complex assembly, seeking compounds that could potentially control neuronal excitability through protein–protein interaction. We first evaluated the effect of MAPKp38 on the assembly of the FGF14:Nav1.6 complex. In the brain MAPKp38 signaling is central for synaptic function and remodeling,[49] and previous studies have shown a role of iFGFs in facilitating the recruitment of MAPKp38δ to the MAPK scaffold IB2/JIP2,[46] a protein involved in axonal transport.[66] The functional significance of the iFGF binding to IB2 is still poorly understood, but one can speculate an implication of the iFGFs for axonal targeting of Nav channels through the IB2/MAPKp38δ complex. Our results show that pretreatment with the p38 inhibitor PD169316, significantly reduces the FGF14:Nav1.6 complex assembly. Interestingly, direct phosphorylation of Nav1.6 by p38 suppresses current density and promotes channel internalization.[67–69] Thus, activation of p38 might lead to opposite effects on neuronal excitability depending on whether it results from direct phosphorylation of Nav1.6 or increased stability of the FGF14:Nav1.6 complex. Additional studies are needed to evaluate the functional significance of this pathway *in vivo*.

We next evaluated the effect of BAY 11-7082, an inhibitor of the NFκB pathway, on the FGF14:Nav1.6 complex assembly. There is an emerging interest for the role of the IKK/NFκB pathway in the brain. In the canonical NFκB activation pathway, the IKK complex phosphorylates the inhibitor of NFκB (IκB), IκBα, leading to its degradation and to the activation of nuclear NFκB.[70] The IKK/NFκB has been implicated in neuronal plasticity,[71,72] neuronal survival and neuronal injury.[73] Interestingly, functional components of the IKK/NFκB signaling cascade are expressed at the AIS of neurons together with members of the iFGF family,[48] contributing to axonal growth and formation of the AIS.[74,75] Some of these effects might result from rapid nongenomic activity of NFκB.[72,76] In this study, we show that inhibition of IKK limits the FGF14:Nav1.6 complex assembly. Thus, stimuli that activate the NFκB pathway *in vivo* might promote the assembly of the Nav channel to its multivalent accessory protein, FGF14, stimulating excitability. How these predicted outcomes correlate with the emerging role of the NFκB pathway in neuronal polarity[74,75] is of great interest and should be investigated. Overall, our findings provide evidence for a dynamic regulation of the FGF14:Nav1.6 channel C-tail complex by two specific kinase pathways, MAPK/p38 and NFκB. A challenging task would be to extend this study to most, if not all, kinases, and more broadly to evaluate the role of phosphorylation-dependent protein–protein interactions in regulating neuronal excitability. One approach to such large-scale studies might be to systematically analyze the effect of kinases inhibitors on all known combinatorial interactions between Nav isoforms and iFGFs or any other relevant accessory proteins through chemical library screenings. Upon upscaling and miniaturization, the LCA could conceivably provide the basis for a rapid and high-throughput methodology toward this long-term goal.

One problem associated with using luciferase-based assays in screening studies is the number of false positives arising from the direct effect of compounds on the enzymatic activity of luciferase. A growing number of studies have reported such effects. A relevant example is PTC124 (3-[5-(2-fluorophenyl)-1,2,4-

oxadiazol-3-yl]benzoic acid), a molecule originally identified in a cell-based firefly luciferase assay as a potential therapeutic agent,[77] which was later discovered to directly suppress the activity of the luciferase reporter.[50,78,79] To validate the effect of PD169316 and BAY 11-1082, we designed a series of counter screenings against the activity of recombinant luciferase, cell viability, and protein expression. To accelerate data validation and triage false positives at early stages, we propose these validation steps to be an integrative platform for any luminescence-based chemical screening.

In summary, we have adapted the LCA to study the assembly of a protein complex at the level of Nav channels. Based on the sensitivity and reliability of this assay, we envision that this study introduces a novel, rapid, and robust methodology for detecting the dynamic regulation of protein–protein interactions within ion channel complexes real-time in live cells with potential applications in the proteomic and drug discovery field. The large network of protein–protein interactions that composes the macromolecular complex around ion channels and controls neuronal function provides a rich source of drugable interfaces.[80,81] The specificity of these interactions is regulated by hot spots, and peptides, peptidomimetics, and small molecules targeting these hot spots can serve as highly selective and potent scaffolds for drug development.[5,82] The LCA is a rapid and effective method that could be employed for compound screening identification, hit validation, and hit-to-lead transition toward drug discovery development against Nav channels and other challenging transmembrane ion channels.[83] The new generation of the split-luciferase reporters based on the heterocomplementation of green and red luciferase[84] extends the capability of the assay to detect three-way combinations of interacting partners, providing even broader possibilities for studying the ion channel interactome.

ACKNOWLEDGMENTS

The authors thank Dr. Sarkar Partha (Department of Neurology, UTMB) for providing the firefly full-length luciferase; Dr. David Piwinca-Worms (Washington University, St. Louis, MO) for the gift of the plasmids expressing FRB-NLuc and FKBP-CLuc; Dr. Benedict Dargent (INSERM, France) for the CD4-Nav1.6 construct; Dr. Van Swieten (Department of Neurology, Erasmus Medical Center, Rotterdam, The Netherlands) for providing the PDB coordinates of the FGF14 molecular model; and Marcy Bubar Jordan (Center for Addiction Research, UTMB) for proofreading the manuscript. This work was supported by a grant from the Institute for Translational Sciences from UTMB (F.L.), a Research Starter grant from the PhRMA Foundation (F.L., S.S.M.), the American Heart Association (S.S.M.), and 5UC7AI07008304 (R.V. and N.B.).

DISCLOSURE STATEMENT

No competing financial interests exist.

REFERENCES

1. Thayer DA, Jan LY: Mechanisms of distribution and targeting of neuronal ion channels. *Curr Opin Drug Discov Devel* 2010;13:559–567.
2. Leterrier C, Brachet A, Fache MP, Dargent B: Voltage-gated sodium channel organization in neurons: protein interactions and trafficking pathways. *Neurosci Lett* 2010: 486:92–100.
3. Catterall WA: Signaling complexes of voltage-gated sodium and calcium channels. *Neurosci Lett* 2010;486:107–116.
4. Berg T: Small-molecule inhibitors of protein-protein interactions. *Curr Opin Drug Discov Devel* 2008;11:666–674.
5. Acuner Ozbabacan SE, Gursoy A, Keskin O, Nussinov R: Conformational ensembles, signal transduction and residue hot spots: application to drug discovery. *Curr Opin Drug Discov Devel* 2010;13:527–537.
6. Catterall WA, Goldin AL, Waxman SG: International Union of Pharmacology. XLVII. Nomenclature and structure-function relationships of voltage-gated sodium channels. *Pharmacol Rev* 2005;57:397–409.
7. Smallwood PM, Munoz-Sanjuan I, Tong P, *et al.*: Fibroblast growth factor (FGF) homologous factors: new members of the FGF family implicated in nervous system development. *Proc Natl Acad Sci USA* 1996;93:9850–9857.
8. Laezza F, Lampert A, Kozel MA, *et al.*: FGF14 N-terminal splice variants differentially modulate Nav1.2 and Nav1.6-encoded sodium channels. *Mol Cell Neurosci* 2009;42:90–101.
9. Goetz R, Dover K, Laezza F, *et al.*: Crystal structure of a fibroblast growth factor homologous factor (FHF) defines a conserved surface on FHFs for binding and modulation of voltage-gated sodium channels. *J Biol Chem* 2009;284: 17883–17896.
10. Laezza F, Gerber BR, Lou JY, *et al.*: The FGF14(F145S) mutation disrupts the interaction of FGF14 with voltage-gated Na+ channels and impairs neuronal excitability. *J Neurosci* 2007;27:12033–12044.
11. Lou JY, Laezza F, Gerber BR, *et al.*: Fibroblast growth factor 14 is an intracellular modulator of voltage-gated sodium channels. *J Physiol* 2005;569:179–193.
12. Goldfarb M, Schoorlemmer J, Williams A, *et al.*: Fibroblast growth factor homologous factors control neuronal excitability through modulation of voltage-gated sodium channels. *Neuron* 2007;55:449–463.
13. Dover K, Solinas S, D'Angelo E, Goldfarb M: Long-term inactivation particle for voltage-gated sodium channels. *J Physiol* 2010;588:3695–3711.
14. Rush AM, Wittmack EK, Tyrrell L, *et al.*: Differential modulation of sodium channel Na(v)1.6 by two members of the fibroblast growth factor homologous factor 2 subfamily. *Eur J Neurosci* 2006;23:2551–2562.
15. Wittmack EK, Rush AM, Craner MJ, Goldfarb M, Waxman SG, Dib-Hajj SD: Fibroblast growth factor homologous factor 2B: association with Nav1.6 and selective colocalization at nodes of ranvier of dorsal root axons. *J Neurosci* 2004;24:6765–6775.
16. Liu CJ, Dib-Hajj SD, Renganathan M, Cummins TR, Waxman SG: Modulation of the cardiac sodium channel Na(v)1.5 by fibroblast growth factor homologous factor 1B. *J Biol Chem* 2003;278:1029–1036.
17. Liu C, Dib-Hajj SD, Waxman SG: Fibroblast growth factor homologous factor 1B binds to the C terminus of the tetrodotoxin-resistant sodium channel rNav1.9a (NaN). *J Biol Chem* 2001;276:18925–18933.
18. Cusdin FS, Clare JJ, Jackson AP: Trafficking and cellular distribution of voltage-gated sodium channels. *Traffic* 2008;9:17–26.
19. Wang C, Wang C, Hoch EG, Pitt GS: Identification of novel interaction sites that determine specificity between fibroblast growth factor homologous factors and voltage gated sodium channels. *J Biol Chem* 2011;286:2453–2463.
20. Brusse E, de Koning I, Maat-Kievit A, Oostra BA, Heutink P, van Swieten JC: Spinocerebellar ataxia associated with a mutation in the fibroblast growth factor 14 gene (SCA27): a new phenotype. *Mov Disord* 2006;21: 396–401.
21. Van Swieten JC, Brusse E, de Graaf BM, *et al.*: A mutation in the fibroblast growth factor 14 gene is associated with autosomal dominant cerebellar ataxia. *Am J Hum Genet* 2003;72:191–199.
22. Shakkottai VG, Xiao M, Xu L, *et al.*: FGF14 regulates the intrinsic excitability of cerebellar Purkinje neurons. *Neurobiol Dis* 2009;33:81–88.

23. Xiao M, Xu L, Laezza F, Yamada K, Feng S, Ornitz DM: Impaired hippocampal synaptic transmission and plasticity in mice lacking fibroblast growth factor 14. *Mol Cell Neurosci* 2007;34:366–377.
24. Kiss L, Bennett PB, Uebele VN, *et al.*: High throughput ion-channel pharmacology: planar-array-based voltage clamp. *Assay Drug Dev Technol* 2003;1:127–135.
25. Masi A, Cicchi R, Carloni A, Pavone FS, Arcangeli A: Optical methods in the study of protein-protein interactions. *Adv Exp Med Biol* 2010;674:33–42.
26. Terstappen GC: Nonradioactive rubidium ion efflux assay and its applications in drug discovery and development. *Assay Drug Dev Technol* 2004;2:553–559.
27. Michnick SW, Ear PH, Manderson EN, Remy I, Stefan E: Universal strategies in research and drug discovery based on protein-fragment complementation assays. *Nat Rev Drug Discov* 2007;6:569–582.
28. Johnsson N, Varshavsky A: Split ubiquitin as a sensor of protein interactions in vivo. *Proc Natl Acad Sci USA* 1994;91:10340–10344.
29. Pelletier JN, Campbell-Valois FX, Michnick SW: Oligomerization domain-directed reassembly of active dihydrofolate reductase from rationally designed fragments. *Proc Natl Acad Sci USA* 1998;95:12141–12146.
30. Galarneau A, Primeau M, Trudeau LE, Michnick SW: Beta-lactamase protein fragment complementation assays as in vivo and in vitro sensors of protein protein interactions. *Nat Biotechnol* 2002;20:619–622.
31. Magliery TJ, Wilson CG, Pan W, *et al.*: Detecting protein-protein interactions with a green fluorescent protein fragment reassembly trap: scope and mechanism. *J Am Chem Soc* 2005;127:146–157.
32. Hu CD, Kerppola TK: Simultaneous visualization of multiple protein interactions in living cells using multicolor fluorescence complementation analysis. *Nat Biotechnol* 2003;21:539–545.
33. Stefan E, Aquin S, Berger N, *et al.*: Quantification of dynamic protein complexes using Renilla luciferase fragment complementation applied to protein kinase A activities in vivo. *Proc Natl Acad Sci USA* 2007;104:16916–16921.
34. Remy I, Michnick SW: A highly sensitive protein-protein interaction assay based on Gaussia luciferase. *Nat Methods* 2006;3:977–979.
35. Luker KE, Smith MC, Luker GD, Gammon ST, Piwnica-Worms H, Piwnica-Worms D: Kinetics of regulated protein-protein interactions revealed with firefly luciferase complementation imaging in cells and living animals. *Proc Natl Acad Sci USA* 2004;101:12288–12293.
36. Rowe L, Dikici E, Daunert S: Engineering bioluminescent proteins: expanding their analytical potential. *Anal Chem* 2009;81:8662–8668.
37. Inglese J, Johnson RL, Simeonov A, *et al.*: High-throughput screening assays for the identification of chemical probes. *Nat Chem Biol* 2007;3:466–79.
38. Garrido JJ, Fernandes F, Giraud P, *et al.*: Identification of an axonal determinant in the C-terminus of the sodium channel Na(v)1.2. *EMBO J* 2001;20:5950–5961.
39. Garrido JJ, Giraud P, Carlier E, *et al.*: A targeting motif involved in sodium channel clustering at the axonal initial segment. *Science* 2003;300:2091–2094.
40. Garrido JJ, Fernandes F, Moussif A, Fache MP, Giraud P, Dargent B: Dynamic compartmentalization of the voltage-gated sodium channels in axons. *Biol Cell* 2003;95:437–45.
41. Pettersen EF, Goddard TD, Huang CC, *et al.*: UCSF Chimera—a visualization system for exploratory research and analysis. *J Comput Chem* 2004;25:1605–1612.
42. Lovell S, Word JM, Richardson JS, Richardson DC: The penultimate rotamer library. *Proteins* 2000;40:389–408.
43. Gregersen N, Bolund L, Bross P: Protein misfolding, aggregation, and degradation in disease. *Methods Mol Biol* 2003;232:3–16.
44. Berendt FJ, Park KS, Trimmer JS: Multisite phosphorylation of voltage-gated sodium channel alpha subunits from rat brain. *J Proteome Res* 2010;9:1976–1984.
45. Bréchet A, Fache MP, Brachet A, *et al.*: Protein kinase CK2 contributes to the organization of sodium channels in axonal membranes by regulating their interactions with ankyrin G. *J Cell Biol* 2008;183:1101–1114.
46. Schoorlemmer J, Goldfarb M: Fibroblast growth factor homologous factors and the islet brain-2 scaffold protein regulate activation of a stress-activated protein kinase. *J Biol Chem* 2002;277:49111–49119.
47. Shao D, Okuse K, Djamgoz MB: Protein-protein interactions involving voltage-gated sodium channels: post-translational regulation, intracellular trafficking and functional expression. *Int J Biochem Cell Biol* 2009;41:1471–1481.
48. Schultz C, König HG, Del Turco D, *et al.*: Coincident enrichment of phosphorylated IkappaBalpha, activated IKK, and phosphorylated p65 in the axon initial segment of neurons. *Mol Cell Neurosci* 2006;33:68–80.
49. Sweatt JD: The neuronal MAP kinase cascade: a biochemical signal integration system subserving synaptic plasticity and memory. *J Neurochem* 2001;76:1–10.
50. Thorne N, Auld DS, Inglese J: Apparent activity in high-throughput screening: origins of compound-dependent assay interference. *Curr Opin Chem Biol* 2010;14:315–324.
51. Herbst KJ, Allen MD, Zhang J: The cAMP-dependent protein kinase inhibitor H-89 attenuates the bioluminescence signal produced by Renilla Luciferase. *PLoS One* 2009;4:e5642.
52. Pierce J, Schoenleber R, Jesmok G, *et al.*: Novel inhibitors of cytokine-induced IkappaBalpha phosphorylation and endothelial cell adhesion molecule expression show anti-inflammatory effects in vivo. *J Biol Chem* 1997;272:21096–21103.
53. Fu Y, O'Connor LM, Shepherd TG, Nachtigal MW: The p38 MAPK inhibitor, PD169316, inhibits transforming growth factor beta-induced Smad signaling in human ovarian cancer cells. *Biochem Biophys Res Commun* 2003;310:391–397.
54. Lazo JS, Brady LS, Dingledine R: Building a pharmacological lexicon: small molecule discovery in academia. *Mol Pharmacol* 2007;72:1–7.
55. Zhang JH, Chung TD, Oldenburg KR: A simple statistical parameter for use in evaluation and validation of high throughput screening assays. *J Biomol Screen* 1999;4:67–73.
56. Wozniak DF, Xiao M, Xu L, Yamada KA, Ornitz DM: Impaired spatial learning and defective theta burst induced ltp in mice lacking fibroblast growth factor 14. *Neurobiol Dis* 2007;1:14–26.
57. Royeck M, Horstmann MT, Remy S, Reitze M, Yaari Y, Beck H: Role of axonal NaV1.6 sodium channels in action potential initiation of CA1 pyramidal neurons. *J Neurophysiol* 2008;100:2361–2380.
58. Craner MJ, Newcombe J, Black JA, Hartle C, Cuzner ML, Waxman SG: Molecular changes in neurons in multiple sclerosis: altered axonal expression of Nav1.2 and Nav1.6 sodium channels and Na+/Ca2+ exchanger. *Proc Natl Acad Sci USA* 2004;101:8168–8173.
59. Craner MJ, Hains BC, Lo AC, Black JA, Waxman SG: Co-localization of sodium channel Nav1.6 and the sodium-calcium exchanger at sites of axonal injury in the spinal cord in EAE. *Brain* 2004;127:294–303.
60. Clutterbuck LA, Posada CG, Visintin C, *et al.*: Oxadiazolylindazole sodium channel modulators are neuroprotective toward hippocampal neurones. *J Med Chem* 2009;52:2694–2707.
61. Madoux F, Li X, Chase P, *et al.*: Potent, selective and cell penetrant inhibitors of SF-1 by functional ultra-high-throughput screening. *Mol Pharmacol* 2008;73:1776–1784.
62. Madoux F, Simanski S, Chase P, *et al.*: An ultra-high throughput cell-based screen for wee1 degradation inhibitors. *J Biomol Screen* 2010;15:907–917.
63. Rusconi R, Combi R, Cestèle S, *et al.*: A rescuable folding defective Nav1.1 (SCN1A) sodium channel mutant causes GEFS+: common mechanism in Nav1.1 related epilepsies? *Hum Mutat* 2009;30:E747–60.
64. Rusconi R, Scalmani P, Cassulini RR, *et al.*: Modulatory proteins can rescue a trafficking defective epileptogenic Nav1.1 Na+ channel mutant. *J Neurosci* 2007;27:11037–11046.
65. Mantegazza M, Gambardella A, Rusconi R, *et al.*: Identification of an Nav1.1 sodium channel (SCN1A) loss-of-function mutation associated with familial simple febrile seizures. *Proc Natl Acad Sci USA* 2005;102:18177–18182.
66. Koushika SP: "JIP"ing along the axon: the complex roles of JIPs in axonal transport. *Bioessays* 2008;30:10–14.
67. Gasser A, Cheng X, Gilmore ES, Tyrrell L, Waxman SG, Dib-Hajj SD: Two Nedd4-binding motifs underlie modulation of sodium channel Nav1.6 by p38 MAPK. *J Biol Chem* 2010;285:26149–26161.

68. Stamboulian S, Choi JS, Ahn HS, *et al.*: ERK1/2 mitogen-activated protein kinase phosphorylates sodium channel Na(v)1.7 and alters its gating properties. *J Neurosci* 2010;30:1637–1647.
69. Hudmon A, Choi JS, Tyrrell L, *et al.*: Phosphorylation of sodium channel Na(v)1.8 by p38 mitogen-activated protein kinase increases current density in dorsal root ganglion neurons. *J Neurosci* 2008;28:3190–3201.
70. Israel A: The IKK complex, a central regulator of NF-kappaB activation. *Cold Spring Harb Perspect Biol* 2010;2:a000158.
71. Lubin FD, Sweatt JD: The IkappaB kinase regulates chromatin structure during reconsolidation of conditioned fear memories. *Neuron* 2007;55:942–957.
72. Boersma MC, Dresselhaus EC, De Biase LM, Mihalas AB, Bergles DE, Meffert MK: A requirement for nuclear factor-κB in developmental and plasticity-associated synaptogenesis. *J Neurosci* 2010;31:5414–5425.
73. Sarnico I, Lanzillotta A, Benarese M, *et al.*: NF-κB dimers in the regulation of neuronal survival. *Int Rev Neurobiol* 2009;85:351–362.
74. Sanchez-Ponce D, Tapia M, Munoz A, Garrido JJ: New role of IKK alpha/beta phosphorylated I kappa B alpha in axon outgrowth and axon initial segment development. *Mol Cell Neurosci* 2008;37:832–844.
75. Sanchez-Ponce D, Munoz A, Garrido JJ: Casein kinase 2 and microtubules control axon initial segment formation. *Mol Cell Neurosci* 2010;46:222–234.
76. Boersma MC, Meffert MK: Novel roles for the NF-κB signaling pathway in regulating neuronal function. *Sci Signal* 2008;1:pe7.
77. Welch EM, Barton ER, Zhuo J, *et al.*: PTC124 targets genetic disorders caused by nonsense mutations. *Nature* 2007;447:87–91.
78. Auld DS, Lovell S, Thorne N, *et al.*: Molecular basis for the high-affinity binding and stabilization of firefly luciferase by PTC124. *Proc Natl Acad Sci USA* 2010;107:4878–4883.
79. Auld DS, Thorne N, Maguire WF, Inglese J: Mechanism of PTC124 activity in cell-based luciferase assays of nonsense codon suppression. *Proc Natl Acad Sci USA* 2009;106:3585–3590.
80. Camerino DC, Desaphy JF: Grand challenge for ion channels: an underexploited resource for therapeutics. *Front Pharmacol* 2010;1:113.
81. Tesmer JJ: Pharmacology. Hitting the hot spots of cell signaling cascades. *Science* 2006;312:377–378.
82. Arkin MR, Wells JA: Small-molecule inhibitors of protein-protein interactions: progressing towards the dream. *Nat Rev Drug Discov* 2004;3:301–317.
83. Brueggemann A, George M, Klau M, *et al.*: Ion channel drug discovery and research: the automated Nano-Patch-Clamp technology. *Curr Drug Discov Technol* 2004;1:91–96.
84. Villalobos V, Naik S, Bruinsma M, *et al.*: Dual-color click beetle luciferase heteroprotein fragment complementation assays. *Chem Biol* 2010;17:1018–1029.

Address correspondence to:
Fernanda Laezza, MD, PhD
Department of Pharmacology & Toxicology
The University of Texas Medical Branch
301 University Boulevard
Galveston, TX 77555

E-mail: felaezza@utmb.edu